

# Chemo- and Regioselective Functionalization of Isotactic Polypropylene: A Mechanistic and Structure–Property Study

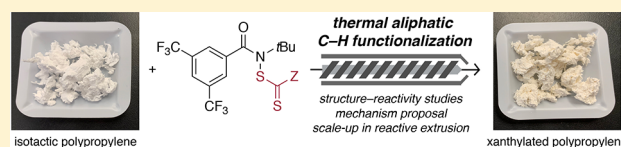
Jill B. Williamson,<sup>†</sup> Christina G. Na,<sup>†</sup> Robert R. Johnson, III,<sup>†</sup> William F. M. Daniel,<sup>‡</sup> Erik J. Alexanian,<sup>\*,†</sup> and Frank A. Leibfarth<sup>\*,†</sup>

<sup>†</sup>Department of Chemistry, The University of North Carolina at Chapel Hill, Chapel Hill, North Carolina 27599, United States

<sup>‡</sup>Department of Applied Physical Sciences, The University of North Carolina at Chapel Hill, Chapel Hill, North Carolina 27599, United States

## Supporting Information

**ABSTRACT:** Polyolefins represent a high-volume class of polymers prized for their attractive thermomechanical properties, but the lack of chemical functionality on polyolefins makes them inadequate for many high-performance engineering applications. We report a metal-free postpolymerization modification approach to impart functionality onto branched polyolefins without the deleterious chain-coupling or chain-scission side reactions inherent to previous methods. The identification of conditions for thermally initiated polyolefin C–H functionalization combined with the development of new reagents enabled the addition of xanthates, trithiocarbonates, and dithiocarbamates to a variety of commercially available branched polyolefins. Systematic experimental and kinetic studies led to a mechanistic hypothesis that facilitated the rational design of reagents and reaction conditions for the thermally initiated C–H xanthylation of isotactic polypropylene (iPP) within a twin-screw extruder. A structure–property study showed that the functionalized iPP adheres to polar surfaces twice as strongly as commercial iPP while demonstrating similar tensile properties. The fundamental understanding of the elementary steps in amidyl radical-mediated polyolefin functionalization provided herein reveals key structure–reactivity relationships for the design of improved reagents, while the demonstration of chemoselective and scalable iPP functionalization to realize a material with improved adhesion properties indicates the translational potential of this method.



## INTRODUCTION

The annual global market for polyolefins is over 150 million metric tons and projected to grow at an annual rate of 6.7% through 2025.<sup>1</sup> The continued demand for these high-volume, low-cost thermoplastics is attributed to their high tensile strength, ductility, thermal stability, and chemical resistance.<sup>2</sup> These excellent thermomechanical properties along with the versatility of polyolefins make them useful in diverse industries, ranging from commodity packaging or automotive applications to the medical device market.<sup>3,4</sup> Despite their omnipresence, these hydrocarbons are hindered by their inability to interface with polar additives, fillers, or other materials.<sup>5</sup> This intrinsic limitation renders polyolefins inadequate for use in many high-performance engineering applications. The addition of polar functionality to polyolefins has been a long-standing goal in polymer chemistry due to the promise of materials that combine the thermomechanical properties of polyolefins with the desirable properties of high-value polymers used in composites, adhesives, and blends.<sup>6,7</sup>

The two most common synthetic approaches in pursuit of polar polyolefins include copolymerization and postpolymerization modification (PPM).<sup>7–10</sup> Methods for the copolymerization of  $\alpha$ -olefins with polar monomers have been pursued aggressively for decades.<sup>7,11,12</sup> An intrinsic problem of installing polarity in this fashion is that Lewis basic comonomers bind strongly to early transition metal catalysts

used for coordination–insertion polymerization and hinder their activity.<sup>6</sup> In response, late transition metal catalysts that are more tolerant to polar functionality have been developed.<sup>5,13,14</sup> Despite significant effort, state-of-the-art methods exhibit insufficient catalyst activity or result in inadequate material properties for translation.<sup>15–19</sup>

The PPM of polyolefins leverages established industrial production capacity while installing a tunable degree of functionality randomly along the polymer backbone. The radical-mediated addition of maleic anhydride to polyethylene (PE) and isotactic polypropylene (iPP) is practiced commercially via reactive extrusion.<sup>20,21</sup> The lack of chemoselectivity in this strategy results in deleterious side reactions including  $\beta$ -scission and polymer chain coupling that adversely affect the molar mass, molecular weight distribution (MWD), and thermomechanical properties of the polymers.<sup>22–25</sup> Consequently, maleic anhydride functionalization of iPP and other branched polyolefins results in low molecular weight species with minimal incorporation of polar functionality.<sup>24,26–28</sup>

A number of modern polyolefin PPM methods have been developed. Metal-catalyzed approaches have been successful,<sup>29–31</sup> most notably the ruthenium-catalyzed hydroxylation

Received: May 30, 2019

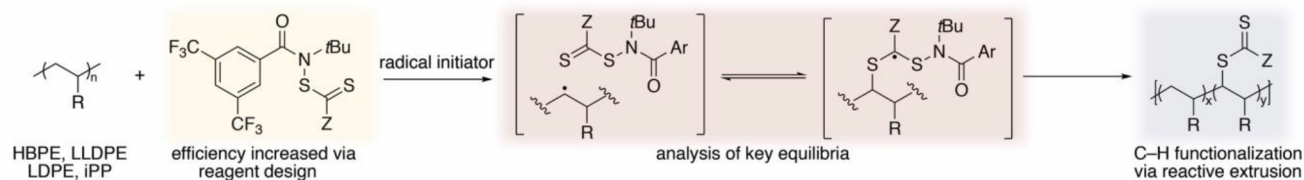


**Figure 1.** Amidyl radical-mediated polyolefin C–H functionalization via thermal initiation.

of branched polyolefins.<sup>32–34</sup> Trace metal in the final material, however, results in oxidative degradation of the polymer sample over time.<sup>35</sup> For this reason, as well as the cost and accessibility challenges associated with precious metals, a metal-free route would be preferred. Previously reported metal-free methods for PPM of polyolefins rely on hydrogen atom abstraction by electron-rich radicals with moderate bond dissociation free energies (BDFEs), resulting in a decrease in the molecular weight for branched polyolefins due to  $\beta$ -scission.<sup>36–39</sup> Furthermore, none of these modern approaches have been optimized for and implemented in an extruder, which is a key requirement for translation.

In an effort to develop a metal-free PPM reaction that retains the beneficial thermomechanical properties of the parent polymer, we recently identified a sterically encumbered *N*-xanthylamide reagent that, upon photolysis, provided regioselective xanthyl group transfer to branched polyolefins without deleterious chain scission reactions. In contrast to previously reported metal-free PPM approaches that rely on radicals generated from the thermal decomposition of peroxides to abstract hydrogen atoms, this reagent did not require an exogenous initiator, which suggests that the transformation proceeds through a fundamentally distinct pathway. The development of a thermal PPM process combined with a deeper understanding of the mechanism of this unique reagent is required to design improved reagents and identify reaction conditions that enable functionalization via reactive extrusion.

Our current mechanistic hypothesis is that an amidyl radical is responsible for hydrogen atom abstraction, followed by rapid trapping of the polymer-centered radical by the thiocarbonyl group of the reagent (Figure 1). This results in a set of complex equilibria that we probe herein through systematic reagent design, crossover experiments, and kinetic studies. The culmination of the data presented provides the rational design of reagents and reaction conditions for the thermally initiated functionalization of branched polyolefins without coincident chain scission. Key principles identified from systematic experiments facilitated the C–H xanthylation of *i*PP within a twin-screw extruder. The resulting functionalized *i*PP demonstrated similar mechanical properties to the virgin polymer while exhibiting twice the adhesion strength to polar substrates. The fundamental understanding of the elementary steps in amidyl radical-mediated polyolefin functionalization provided in this report reveals key structure–reactivity relationships and serves as a platform for the design of improved methods and translational technologies for polymer C–H functionalization.

## RESULTS AND DISCUSSION

**Structure–Reactivity Studies of Amidyl Reagents.** To develop structure–reactivity relationships for the thermally initiated C–H functionalization, cyclooctane was chosen as a

small-molecule surrogate to facilitate rapid and accurate characterization. Heating cyclooctane to 80 °C in benzene (0.15 M) with xanthylamide **1a** and 10 mol % azobis(isobutyronitrile) (AIBN) successfully yielded xanthylated cyclooctane in a 22% yield (Figure 2). These conditions

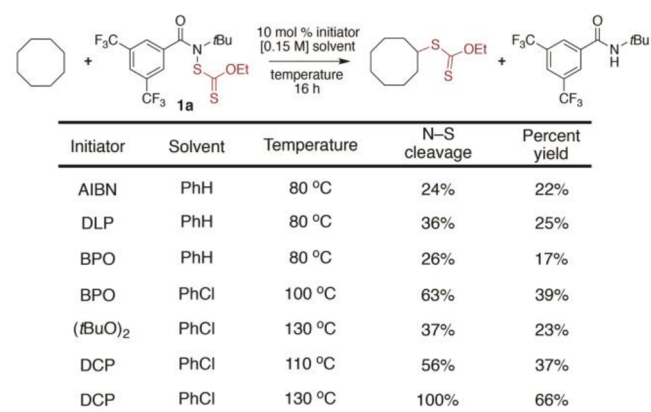


**Figure 2.** Optimization of the thermally initiated xanthylation of cyclooctane with **1b**. (*t*BuO)<sub>2</sub> = di-*tert*-butyl peroxide. N–S cleavage and percent yield were determined by <sup>1</sup>H NMR analysis using hexamethyldisiloxane as an internal standard.

resulted in only 24% homolysis of the N–S bond in **1a**, which was monitored by conversion of **1a** to its respective parent amide by <sup>1</sup>H NMR. Alternative radical initiators, such as dilauroyl peroxide (DLP) and benzoyl peroxide (BPO), yielded similar results at 80 °C. In the case of BPO, increasing the reaction temperature resulted in an increase in yield. Further optimization found that the reaction performed best with dicumyl peroxide (DCP) at 130 °C. Upon product isolation, only xanthylated cyclooctane, *O,O*-diethyl dithio bis(thioformate), and the parent amide were observed. This chemoselective C–H functionalization is attractive for translation to polymer substrates, since multiple products attached to the same polymer chain cannot be separated from one another.<sup>11</sup>

The electronic properties of thiocarbonylthio functional groups are known to play a large role in their reactivity. For example, these groups demonstrate different rates of chain transfer in reversible addition–fragmentation chain-transfer (RAFT) radical polymerization.<sup>40–43</sup> To probe the structure–reactivity properties of amidyl reagents with different thiocarbonylthio groups, we designed and synthesized **1a–c** (Figure 3).<sup>44–46</sup> Similar to RAFT polymerization, thiocarbonylthio groups can be conveniently described with respect to their *Z* groups: –OEt for **1a**, –SEt for **1b**, and –NEt<sub>2</sub> for **1c**. Despite differing only in the heteroatom of the *Z* group, reagents **1b** and **1c** provided lower yields of functionalized cyclooctane under analogous conditions to those of **1a**. Trithiocarbonylthio **1b** was observed to undergo complete

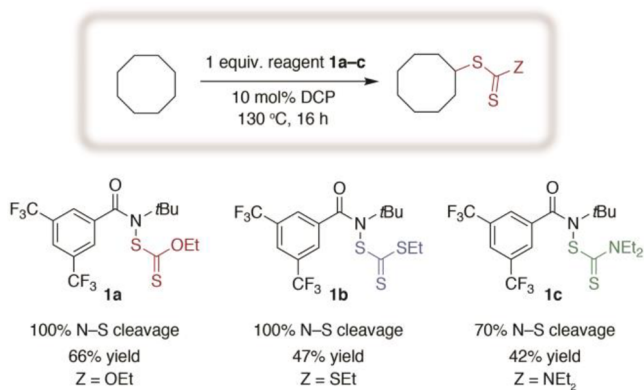


**Figure 3.** Reagents **1a–c** demonstrate initial structure–reactivity relationships for cyclooctane C–H functionalization. N–S cleavage and percent yield were determined by <sup>1</sup>H NMR analysis using hexamethyldisiloxane as an internal standard.

N–S cleavage of **1b** to parent amide, but only a 47% yield of trithiocarbonylated cyclooctane was obtained. Dithiocarbamylamide **1c** did not completely convert to parent amide, but demonstrated a similar yield to that of reagent **1b**.

**Functionalization of Polyolefins.** To translate the results on cyclooctane to polymeric substrates, hyperbranched polyethylene (HBPE) was chosen as a model branched polyolefin for reaction optimization. HBPE with 10 methyl branches per 100 carbons was synthesized using a previously reported Pd(II)  $\alpha$ -diimine catalyst.<sup>47</sup> Polymers with different number-average molar mass ( $M_n$ ) and narrow dispersities ( $\mathcal{D}$ ) were synthesized in order to determine the influence of reaction conditions on molecular weight and MWD. The use of amorphous HBPE enabled facile characterization of a branched polyolefin at room temperature. Under homogeneous conditions, HBPE was heated at 130 °C for 6–24 h in the presence of **1a–c** and 10 mol % DCP in chlorobenzene at a concentration of 0.2 M with respect to reagent (Figure 4). The stoichiometry of reagents **1a–c** was varied relative to the repeat unit, with functionalization reported as mol % compared to the polymer repeat unit (Figure 4).

$\text{Hyperbranched} + \text{1a-c} \xrightarrow[130\text{ }^\circ\text{C, PhCl}]{10\text{ mol\% DCP}} \text{Hyperbranched-S-C(=S)-Z}$

Entry	Z	Theoretical mol % funct <sup>a</sup>	Actual mol % funct <sup>a</sup>	Conv. of 1a–c <sup>a</sup>	Before <sup>b</sup> $M_n$	Before <sup>b</sup> $\mathcal{D}$	After <sup>b</sup> $M_n$	After <sup>b</sup> $\mathcal{D}$
1	–OEt	10	4	80	35	1.03	48	1.11
2	–OEt	20	5	82	35	1.03	51	1.07
3	–OEt	50	7	69	35	1.03	53	1.09
4	–OEt	100	7	54	35	1.03	40	1.07
5	–SET	10	3	50	42	1.05	45	1.12
6	–SET	20	3	35	42	1.05	45	1.08
7	–SET	50	3	39	42	1.05	45	1.06
8	–SET	100	3	32	42	1.05	43	1.10
9	–NEt <sub>2</sub>	10	1	24	35	1.17	35	1.22
10	–NEt <sub>2</sub>	20	1	22	35	1.17	35	1.28
11	–NEt <sub>2</sub>	50	1	21	35	1.17	35	1.27
12	–NEt <sub>2</sub>	100	1	18	35	1.17	36	1.24

**Figure 4.** Reagents **1a–c** were reacted with HBPE in the presence of DCP. <sup>a</sup>Determined by <sup>1</sup>H NMR in CDCl<sub>3</sub>. <sup>b</sup>Determined by SEC against polystyrene standards in tetrahydrofuran.

Polymer C–H functionalization was quantified by <sup>1</sup>H NMR integration of the methylene protons of the Z group (Figure 5A). Theoretical maximum functionalization represents the

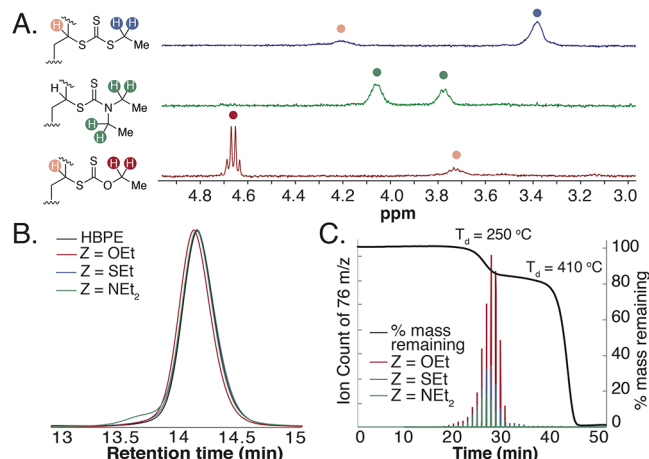


**Figure 5.** (A) <sup>1</sup>H NMR of 1 mol % functionalized HBPE was taken in CDCl<sub>3</sub> and used to determine percent functionalization. The methine proton of dithiocarbamylated HBPE likely overlaps with the methylene protons of the diethylamine Z group. (B) SEC traces obtained by the refractive index detector of 1 mol % functionalized HBPE; (C) TGA–MS of HBPE.

stoichiometry of reagent relative to repeat unit (i.e., a theoretical maximum of 10 mol % functionalization is addition of 1 equiv of reagent per 10 repeat units). Exposing HBPE along with reagent **1a** at a theoretical maximum functionalization of 10 mol % resulted in 4 mol % polymer xanthylation (entry 1, Figure 4). By increasing the mol % theoretical maximum xanthylation, C–H functionalization of HBPE proved tunable in a range of 1–7 mol %.

Despite the addition of more reagent, the ultimate mol % functionalization plateaued around 8 mol % for reagent **1a**. Reagents **1b** and **1c** also successfully functionalized HBPE, but the plateau of functionalization appeared at 3 and 1 mol %, respectively. This plateau is in part due to differences in the conversion of **1a–c** to the parent amide, with lower conversion being observed through the series **1a–c** (Figure 4). We note that even low degrees of functionalization can have a significant influence on the structure and properties of a high molecular weight polymer; for example, 1 mol % functionalization installs an average of 9 thiocarbonylthio groups on a polymer chain with an  $M_n$  of 25 kg/mol. In agreement with previous work, regioselectivity of amidyl radical hydrogen atom transfer (HAT) was determined by <sup>1</sup>H NMR to be selective toward secondary carbon sites on HBPE.<sup>48,49</sup>

Changes in the MWD were analyzed by size exclusion chromatography (SEC). A sample of HBPE was functionalized with 1 mol % of each of the thiocarbonylthio groups, and the SEC trace of the polymers is shown in Figure 5B. Xanthylated (from **1a**) and trithiocarbonylated (from **1b**) HBPE demonstrate MWD similar to that of the parent polymer, but dithiocarbamylated (from **1c**) HBPE shows evidence of polymer-chain coupling reactions, with a peak appearing at a 13.6 min retention time upon functionalization (Figure 5B).

To assess the influence of the Z group on polymer thermal properties, 1 mol % functionalized HBPE of each Z group variant was analyzed via thermal gravimetric analysis (TGA) and differential scanning calorimetry (DSC). All the polymers

demonstrated thermal stability up to 250 °C, at which point they underwent a partial mass loss before reaching a plateau and fully degrading at >400 °C (Figure 5C). We hypothesized that this partial mass loss was the result of a Chugaev-type elimination.<sup>50,51</sup> To support this hypothesis, the evolution of volatile compounds accompanying the partial mass loss was analyzed by mass spectrometry (TGA/MS). A prominent peak at a mass to charge ( $m/z$ ) of 76.1 was evident in all of the samples, which we hypothesize is due to expulsion of carbon disulfide. On the basis of these data, we hypothesize the thiocarbonylthio groups are undergoing a [1,5]-sigmatropic Chugaev-like rearrangement to yield an olefin on the polymer backbone (Figure S9).<sup>52</sup> This hypothesis is also supported by the magnitude of mass loss for each of the functional polymers in TGA, which correlates to the loss of the entire thiocarbonylthio functional group. The DSC spectra for functional HBPE demonstrate that, with identical degrees of functionalization, the Z groups did not have a significant impact on the thermal properties. The parent polymer underwent glass transition at -69 °C, while the HBPEs with 1 mol % functionalization had glass transition temperatures ( $T_g$ ) of -66 and -67 °C (Figure S5A). HBPE also demonstrates a melting temperature at -42 °C, which does not change considerably upon 1 mol % functionalization. This melting exotherm, however, does disappear at higher mol % functionalization of xanthate and trithiocarbonate (Figure S5B).

**Crossover and Kinetic Experiments.** The structure–reactivity experiments for polymer functionalization (Figure 4) revealed key differences among the three reagents. One of the most instructive was that each reagent reached a maximum mol % functionalization despite further addition of reagent relative to polymer repeat unit. For example, reagent **1a** achieved 8 mol % xanthylation of HBPE when adding 50 mol % reagent, but doubling the amount of reagent did not further increase functionalization. In the case of **1c**, the maximum amount of dithiocarbamylation plateaued at 1 mol % regardless of reagent stoichiometry. We observed a similar trend in our previous work using a photochemical initiation strategy.<sup>48</sup> We hypothesized that this phenomenon was the result of degenerative chain transfer of the thiocarbonylthio groups between polymer chains.<sup>53,54</sup> The equilibria of this chain-transfer process, therefore, would result in reversible functionalization.

To test this hypothesis, we designed and conducted a number of crossover experiments using polymer samples that had previously been functionalized with thiocarbonylthio groups. Initially, an HBPE sample with 5.4 mol % xanthylation was heated in the presence of DCP as an initiator with no additional reagent. A decrease in functionalization to 2.3 mol % was observed (Figure 6A, entry 1). Subsequently, reagents containing Z groups not found on the functionalized polymer (**1b** and **1c**, respectively) were reacted with xanthylated HBPE (Figure 6A, entries 2, 3). In both cases, the mol % functionalization of xanthate decreased and the other thiocarbonylthio group was added to the polymer. The same trends were observed if the HBPE was initially functionalized with trithiocarbonate (entry 4) or dithiocarbamate (entry 5). These experiments demonstrate that polymer functionalization is reversible under the reaction conditions and the ultimate mol % functionalization is affected by the rate of degenerative chain transfer.

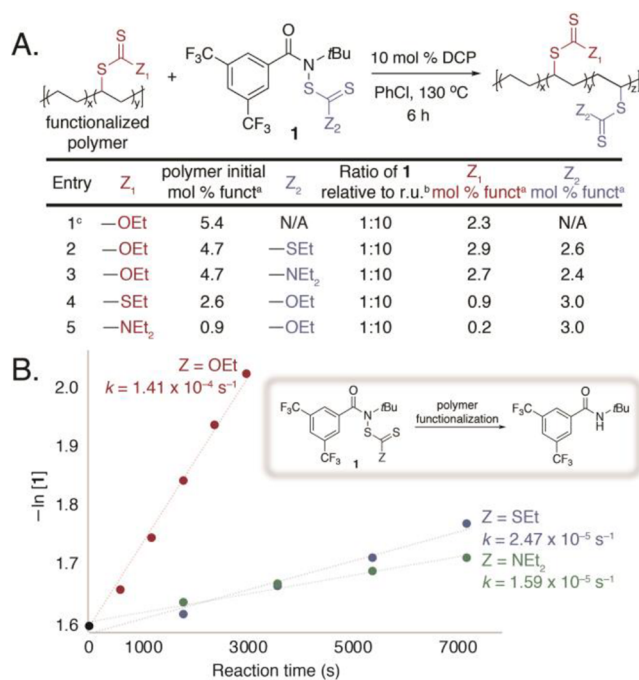


**Figure 6.** (A) Functionalized HBPE was resubjected to the reaction conditions with an amide reagent, yielding polyolefins with two different thiocarbonylthio moieties appended. <sup>a</sup>Determined by <sup>1</sup>H NMR in CDCl<sub>3</sub>. <sup>b</sup>Repeat unit. <sup>c</sup>No functionalized amide reagent was added to the reaction. (B) Kinetics of reagent conversion during functionalization of HBPE at a theoretical maximum of 10 mol % functionalization (10 mol % DCP, 130 °C, [0.2 M] in chlorobenzene). Reaction progress was determined by <sup>1</sup>H NMR.

The observation of reversible functionalization under the reaction conditions led us to probe the kinetics of group transfer for reagents **1a–c** under the reaction conditions. A solution of HBPE, reagent **1**, and DCP in chlorobenzene was separated into aliquots and reacted for different amounts of time to monitor the conversion of **1a–c** to the parent amide. As shown in Figure 6B, reagent **1a** demonstrated considerably faster conversion than that of either **1b** or **1c**, resulting in a rate constant of 9 times and 6 times larger, respectively. The trend for rate of reagent consumption does follow the pattern of mol % polymer functionalization, with reagent **1a** demonstrating both the fastest rate and highest mol % polymer functionalization and **1c** representing the slowest rate and lowest mol % functionalization.

**Mechanistic Hypothesis.** To develop a more comprehensive understanding of this C–H functionalization method, our experimental observations were used to formulate a mechanistic hypothesis (Figure 7). Supported by previous literature, we hypothesize that thermolysis of dicumyl peroxide yields a methyl radical,<sup>55,56</sup> which is quickly trapped by the functionalized amide reagent to form the captodatively stabilized radical **2**. Fragmentation of intermediate **2** yields amidyl radical **4**.<sup>44</sup> We hypothesize that **4** is responsible for HAT from the polymer backbone. HAT of aliphatic C–H bonds by amidyl radicals is exergonic due to the large difference in BDFE of an amidyl radical (BDFE of 107–110 kcal/mol) relative to C–H bonds (BDFE of 96–100 kcal/mol).<sup>57</sup> Furthermore, polarity matching between the electrophilic amidyl radical and electron-rich aliphatic C–H bonds is proposed to lower the kinetic barrier toward HAT.<sup>58,59</sup>

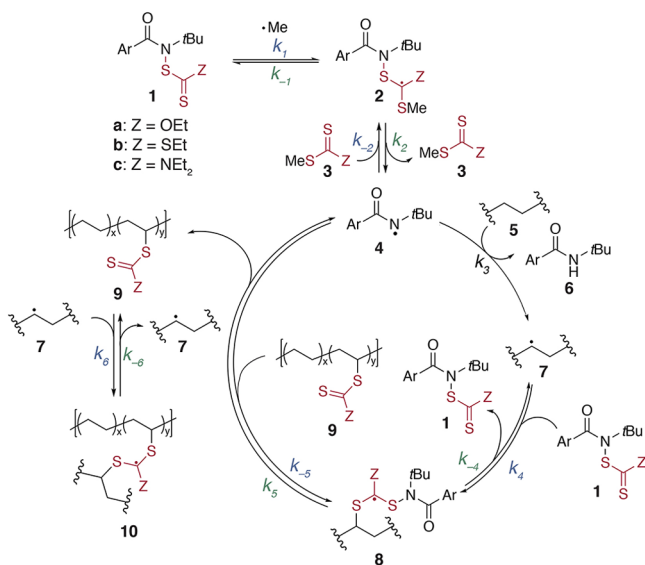


**Figure 7.** Proposed mechanism of amidyl radical-mediated polyolefin C–H functionalization. Polymer side chains were omitted for clarity.

A hydrogen atom from polymer 5 undergoes HAT to furnish the parent amide 6 concomitant with carbon-centered radical 7. The production of 6 was monitored (Figure 6B) to determine the overall rate of conversion of 1 → 6 (Figure 6B). We hypothesize that step 3 is an irreversible transformation due to the thermodynamics of this step. In the productive reaction pathway, carbon-centered radical 7 reacts with reagent 1 to form the captodative radical 8. Fragmentation of 8 is not degenerative, and, based on the kinetic experiments, the rate of fragmentation depends largely on the Z group. C–S homolysis can revert compound 8 back to the carbon-centered radical 7 ( $k_{-4}$ ) or facilitate productive cleavage of intermediate 8 to yield functionalized polymer (9) and amidyl radical 4 ( $k_{-5}$ ). The crossover experiments detailed in Figure 6A demonstrate that both trapping of the polymer-centered radical (7 → 8) and fragmentation to yield functionalized polymer (8 → 9) are reversible. Even after formation of desired product 9, the functionalized polymer can react with amidyl radical 4 and revert back to the carbon-centered radical 7 ( $k_{-5}$ ). It should be noted that, despite the myriad of radical chain-transfer processes occurring in the system, we did not observe cross-linked material in any of the experiments with HBPE.

In a separate experiment, we isolated xanthylated HBPE and added a radical initiator in the presence of a lower molecular weight polyolefin (Figure S6). After the reaction, both polymers exhibited UV–vis absorptions consistent with xanthate functionalization, indicating xanthate group transfer. From this experiment we confirmed that an “off-cycle” degenerative radical chain-transfer process is likely occurring that sequesters a portion of the polymer-centered radical into intermediate 10. Furthermore, control experiments conducted by irradiation of reagents 1a–c excluding the polymer substrate demonstrated that there is most likely a self-immolative radical chain-process that consumes a portion of the reagent without participating in HAT from the polymer (Figure S10). The culmination of these experiments describes the complexity of this C–H functionalization reaction and the many equilibria that must be considered when optimizing reactivity and/or designing new reagents.

Previous work understanding the rate of chain transfer of thiocarbonylthio groups in RAFT polymerization helps to conceptualize the experimental observations.<sup>60,61</sup> In RAFT polymerization, the choice of Z groups had pronounced effects on the rates of radical addition to thiocarbonylthio functional groups and the rate of fragmentation of the captodatively stabilized species.<sup>40</sup> For the Z groups studied herein, the rate of radical addition ( $k_1$ ,  $k_{-2}$ ,  $k_4$ ,  $k_{-5}$ , and  $k_6$ ) decreases in the series SET > OEt > NEt<sub>2</sub>, whereas the rate of radical fragmentation ( $k_{-1}$ ,  $k_2$ ,  $k_{-4}$ ,  $k_5$ , and  $k_{-6}$ ) decreases in the series NEt<sub>2</sub> > OEt > SET (Figure 8). For the dithiocarbamate functional group in 1c,

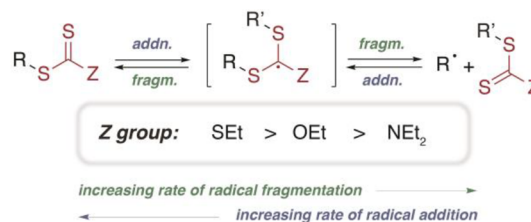


**Figure 8.** Relative rates of radical addition and fragmentation help conceptualize experimental observations for polyolefin C–H functionalization.

we hypothesize that the slower rate of radical addition leads to a longer lifetime of the polymer-centered radical 7 and an increased potential for radical–radical coupling. Significant chain coupling observed in the SEC traces (Figure 5B) supports this hypothesis. The trithiocarbonate group in 1b presumably results in an increase in both  $k_4$  and  $k_{-5}$ . The faster rate of radical addition leads to better control over the MWD of the functionalized polyolefin, which agrees with our experimental results. The faster rate of addition, however, results in a lower amount of overall polymer functionalization than 1a even at high reagent loadings, presumably due to a faster rate for  $k_{-5}$  even after product 9 is formed. We hypothesize that the reagent 1a is successful because it balances the rates of addition and fragmentation. In the conditions described herein, this enables the addition of 8 mol % xanthyl groups to HBPE.

**Functionalization of Semicrystalline Branched Polyolefins.** With a more complete understanding of reagent design principles and reaction mechanism, the thermal functionalization of commercially available semicrystalline branched polyolefins was explored (Figure 9). Reactions were conducted at 180 °C, a temperature typically used for the commercial PPM of polyolefins via reactive extrusion.<sup>62–65</sup> Xanthylation of Dow DNDA-1081 NT 7 linear low density polyethylene resin (LLDPE, 19 branches per 100 carbons) using reagent 1a resulted in 3 mol % functionalization upon addition of 5 mol % of the reagent. At higher equivalents of reagent 1a, mol % functionalization increased along with an observed increase in MWD. On the basis of the mechanistic understanding gained herein, we hypothesized that reagent 1b, which has a faster rate of radical addition, would decrease the amount of deleterious chain coupling and chain scission side reactions. The experimental results confirmed our hypothesis; trithiocarbonate reagent 1b led to moderate functionalization of LLDPE without significantly altering  $M_n$  or the  $\bar{D}$ .

Functionalization of Dow polyethylene 4012 low density (LDPE, 49 branches per 100 carbons) is challenging due to its undefined structure and broad MWD ( $\bar{D}$  = 9.54). Regardless, the trends observed in our mechanistic experiments held true,

Polyolefin	Z	Solvent	Ratio of 1 : r.u. <sup>a</sup>	mol % funct <sup>b</sup>	Before <sup>c</sup> M <sub>n</sub>	Before <sup>c</sup> Đ	After <sup>c</sup> M <sub>n</sub>	After <sup>c</sup> Đ	T <sub>m</sub> <sup>d</sup>
 linear low density PE T <sub>m</sub> = 122 °C	-OEt	DCB	1:20	3	22	3.37	28	7.66	95
	-OEt	DCB	1:10	7	22	3.37	15	6.17	75
	-SEt	DCB	1:10	3	22	3.37	23	3.84	100
	-NEt <sub>2</sub>	DCB	1:10	0	—	—	—	—	—
 low density PE T <sub>m</sub> = 105 °C	-OEt	DCB	1:20	3	41	9.54	41	23.35	84
	-OEt	DCB	1:10	5	41	9.54	39	13.15	73
	-SEt	DCB	1:10	3	41	9.54	43	17.94	85
	-NEt <sub>2</sub>	DCB	1:10	0	—	—	—	—	—
 isotactic PP T <sub>m</sub> = 155 °C	-OEt	DCB	1:20	0	—	—	—	—	—
	-OEt	DCB	1:10	1	64	4.84	84	4.03	144
	-OEt	neat	1:20	1	64	4.84	63	9.72	137
	-OEt	neat	1:10	2	64	4.84	79	7.34	130

— indicates not applicable

**Figure 9.** Functionalization of commercial branched polyolefins. <sup>a</sup>Repeat unit. <sup>b</sup>Determined by <sup>1</sup>H NMR at 110 °C. <sup>c</sup>Determined by SEC at 120 °C. <sup>d</sup>Determined by DSC in the second heating cycle.

with reagent **1a** providing more efficient functionalization. The chemoselective functionalization provided by these reagents is notable, as even small amounts of chain coupling side reactions are known to cause gelation on substrates with high weight-average molecular weights ( $M_w$ ). No functionalization was imparted using reagent **1c**, consistent with results on the HBPE model system.

Basell Profax 6301 polypropylene homopolymer (*i*PP) represents the most challenging semicrystalline polyolefin substrate for C–H functionalization, as it has a high melting temperature, high degree of crystallinity, high branch content (50 methyl branches per 100 carbons), and is prone to  $\beta$ -scission reactions. For this challenging substrate, polymer functionalization in solution was not observed in any of the conditions we tested using reagents **1a–c**. Using reagent **1a** under neat conditions (i.e., without solvent), however, resulted in 1 mol % xanthylation at a theoretical maximum functionalization of 5 mol %. High-temperature <sup>1</sup>H NMR spectroscopy indicated that functionalization was highly regioselective for the primary C–H bonds on *i*PP. Most importantly, no evidence of  $\beta$ -scission of *i*PP was observed and the material maintained a high melting temperature.

The culmination of mechanistic experiments, structure–reactivity studies, and functionalization experiments led us to design conditions for the functionalization of *i*PP by reactive extrusion. A powder formulation of *i*PP mixed with reagent **1a** and 10 mol % DCP at a stoichiometry corresponding to a theoretical maximum functionalization of 5 mol % was injected into a twin-screw extruder at 180 °C and allowed to circulate for 30 min. The extrusion process resulted in the C–H functionalization of *i*PP with 1 mol % xanthate groups and no observed  $\beta$ -scission (Figure 10B). In fact, the shear mixing provided by the twin-screw extruder led to an MWD that better represented that of the parent *i*PP than analogous reactions conducted using mechanical stirring alone (Figure S16).<sup>21</sup>

Scaling up the functionalization in an extruder achieved multigram quantities of xanthylated *i*PP and provided sufficient material for further structure–property evaluation. Prior to further analysis, the xanthylated *i*PP was precipitated to

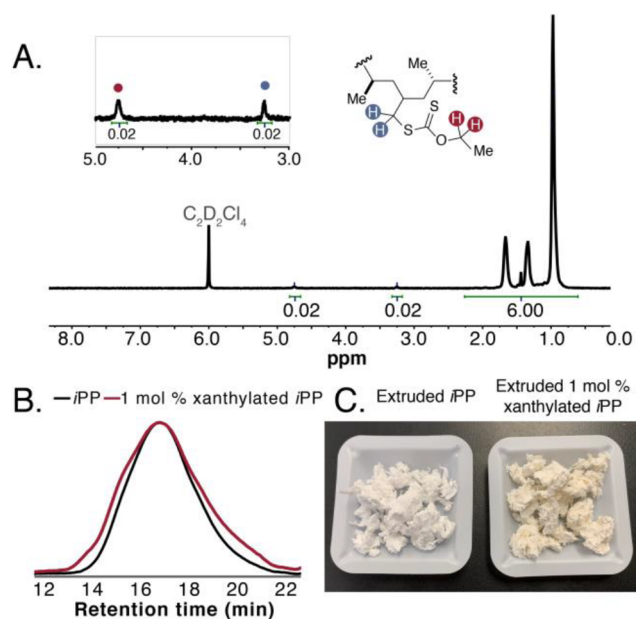


**Figure 10.** Reactive extrusion of *i*PP with reagent **1a** yielded *i*PP with 1 mol % xanthate functionality. The polymer was characterized by (A) <sup>1</sup>H NMR at 110 °C in C<sub>2</sub>D<sub>2</sub>Cl<sub>4</sub> and (B) SEC at 120 °C in trichlorobenzene. (C) Visualization of the large-scale functionalization of *i*PP by reactive extrusion.

remove small-molecule impurities. The crystalline nature of xanthylated *i*PP was confirmed by DSC. The xanthylated *i*PP had a high melting point (137 °C) and a percent crystallinity of 28%. Both of these values are modest decreases from the commercial Profax 6301 material tested under analogous conditions ( $T_m$  = 155 °C, 41% crystalline), which is commonly observed for semicrystalline polymers upon functionalization.<sup>30,33</sup>

The large thermal processing window (above the  $T_m$  and below the  $T_d$ ) of the xanthylated *i*PP enabled us to melt-press films of the material to probe the impact of functionalization on mechanical and adhesive properties. Tensile testing of dog-bone-shaped samples cut from melt-pressed films of the parent Basell Profax 6301 *i*PP and 1 mol % xanthylated *i*PP by dynamic mechanical analysis in linear film tension mode yielded stress–strain curves that showed plastic deformation behavior consistent with semicrystalline thermoplastics (Figure 11A). All quantitative values reported are an average of three or more samples. The yield strength ( $\sigma_y$ ) of *i*PP ( $\sigma_y$  = 35 ± 1 MPa) was slightly higher than that of xanthylated *i*PP ( $\sigma_y$  = 26 ± 3 MPa). The elongation at break value of *i*PP ( $\epsilon_B$  = 570 ± 50%) was congruent with results with xanthylated *i*PP ( $\epsilon_B$  = 430 ± 120%). Strain stiffening was observed in films of *i*PP and xanthylated *i*PP, generating a stress at break of  $\sigma_B$  = 31 ± 2 MPa and  $\sigma_B$  = 24 ± 6 MPa, respectively.

In addition to retaining the desirable thermomechanical properties of commercial polyolefin materials, we expected xanthylated *i*PP to exhibit significantly different adhesive properties due to the intrinsic polarity of the xanthate group. On this basis, we reasoned that xanthylated *i*PP should display superior adhesion to polar surfaces (i.e., glass) relative to polyolefin materials. To test this hypothesis, we prepared a single-lap joint between two glass slides, using *i*PP or xanthylated *i*PP, and subjected it to lap shear analysis (Figure 11B). Xanthylated *i*PP demonstrated more than twice the

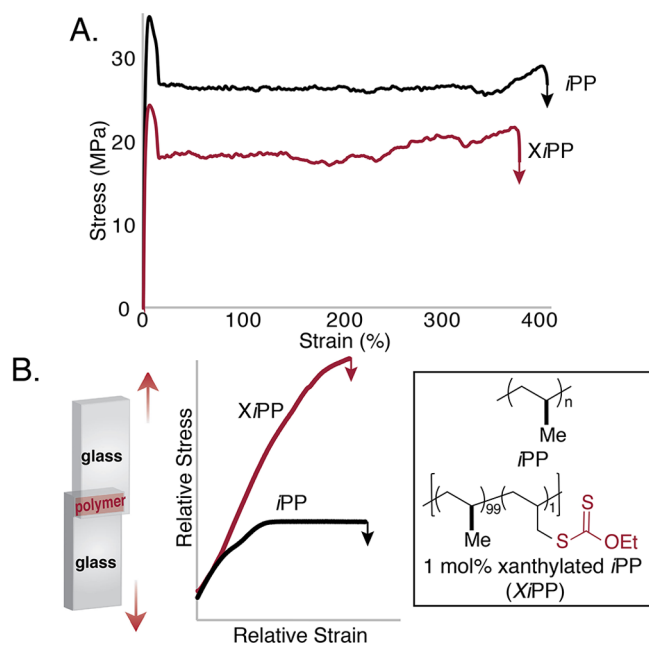


**Figure 11.** Structure–property studies of *i*PP and 1 mol % xanthylated *i*PP (*Xi*PP). (A) Representative stress–strain curves for *i*PP and *Xi*PP measured by tensile testing (0.1 mm/s, room temperature, break point indicated by arrow). (B) Representative relative shear stress–strain curves for *i*PP and *Xi*PP single-lap joints measured by tensile testing (5 mm/min, room temperature).

adhesion strength to glass than did the *i*PP material, with apparent lap shear strengths of  $120 \pm 30$  and  $48 \pm 4$  MPa, respectively. These results prove the significant impact of adding even small amounts of polar functionality onto polyolefins.

## CONCLUSION

A thermally initiated, metal-free C–H functionalization of branched polyolefins is demonstrated using thiocarbonylthio amide reagents. Comprehensive experimental studies on both small molecule and polyolefin substrates revealed key structure–reactivity relationships. Crossover and kinetic experiments provide information on the many competing equilibria that combine to determine the efficiency and magnitude of polymer functionalization. From these experimental studies, we developed a mechanistic hypothesis that informed the translation of these reagents for the successful chemoselective functionalization of commercial samples of semicrystalline polyolefins. Ultimately, the reactive extrusion of *i*PP on a decagram scale was demonstrated and resulted in functionalized *i*PP that adheres to polar substrates twice as strong as commercial *i*PP. We envision the results of this experimental and mechanistic study will serve as a comprehensive launching point for the continued improvement and implementation of polyolefin C–H functionalization in practical settings.

## ASSOCIATED CONTENT

### Supporting Information

The Supporting Information is available free of charge on the ACS Publications website at DOI: 10.1021/jacs.9b05799.

Experimental procedures and spectral data for all new compounds (PDF)

## AUTHOR INFORMATION

### Corresponding Authors

\*[ej@email.unc.edu](mailto:ej@email.unc.edu)

\*[FrankL@email.unc.edu](mailto:FrankL@email.unc.edu)

### ORCID

Erik J. Alexanian: 0000-0002-0256-2133

Frank A. Leibfarth: 0000-0001-7737-0331

### Notes

The authors declare no competing financial interest.

## ACKNOWLEDGMENTS

This work is supported by the Air Force Office of Scientific Research under the Young Investigator Program (#17RT0487). J.B.W. thanks the Henry G. Luce Foundation and UNC for a Clare Boothe Luce Graduate Student Fellowship. C.G.N. thanks the NSF for a Graduate Research Fellowship and the Graduate School for a Royster Fellowship. A provisional patent application has been filed (U.S. Prov.62/567,460). We acknowledge the Polymer and Molecular Characterization Facility in the Center for the Science and Technology of Advanced Materials and Interfaces (STAMI) at the Georgia Institute of Technology (Atlanta, GA, USA) for the high-temperature gel permeation chromatography. This work made use of the Integrated Molecular Structure Education and Research Center (IMSERC) at Northwestern University with thermal analysis with tandem mass spectrometry (TGA–MS) results. We thank Prof. Theo Dingemans and Dr. Maruti Hedge for thoughtful discussions.

## REFERENCES

- Grand View Research. Polyolefin Market Size, Share & Trends Analysis By Product Type (PE, PP, Ethylene Vinyl Acetate, Thermoplastic Olefin), By Application (Film & Sheet, Injection Molding, Blow Molding, Profile Extrusion), and Segment Forecasts, 2018–2025; 2018.
- Galli, P.; Vecellio, G. Polyolefins: The most promising large-volume materials for the 21st century. *J. Polym. Sci., Part A: Polym. Chem.* **2004**, *42* (3), 396–415.
- Seymour, R. B. *History of Polyolefins: The World's Most Widely Used Polymers*; D. Reidel: Dordrecht, 1986.
- Tolinski, M. *Additives for Polyolefins*, 2nd ed.; William Andrew Publishing, 2015.
- Domski, G. J.; Rose, J. M.; Coates, G. W.; Bolig, A. D.; Brookhart, M. Living alkene polymerization: New methods for the precision synthesis of polyolefins. *Prog. Polym. Sci.* **2007**, *32* (1), 30–92.
- Chung, T. C. Synthesis of functional polyolefin copolymers with graft and block structures. *Prog. Polym. Sci.* **2002**, *27* (1), 39–85.
- Boaen, N. K.; Hillmyer, M. A. Post-polymerization functionalization of polyolefins. *Chem. Soc. Rev.* **2005**, *34* (3), 267.
- Franssen, N. M. G.; Reek, J. N. H.; De Bruin, B. A different route to functional polyolefins: Olefin-carbene copolymerisation. *Dalton Trans* **2013**, *42* (25), 9058–9068.
- Vasile, C. *Handbook of Polyolefins*, 2nd ed.; CRC Press: New York, 2000.
- Aima'adeed, A.-A.; Krupa, I. *Polyolefin Compounds and Materials: Fundamentals and Industrial Applications*; Springer International Publishing, 2016.
- Williamson, J. B.; Lewis, S. E.; Johnson III, R. R.; Manning, I. M.; Leibfarth, F. C-H Functionalization of Commodity Polymers. *Angew. Chem., Int. Ed.* **2019**, *58*, 8654–8668.
- Dong, J. Design and synthesis of structurally well-defined functional polypropylenes via transition metal-mediated olefin polymerization chemistry. *Front. Chem. China* **2006**, *1* (2), 145–157.

- (13) Carrow, B. P.; Nozaki, K. Synthesis of Functional Polyolefins Using Cationic Bisphosphine Monoxide–Palladium Complexes. *J. Am. Chem. Soc.* **2012**, *134* (21), 8802–8805.
- (14) Nakamura, A.; Ito, S.; Nozaki, K. Coordination-Insertion Copolymerization of Fundamental Polar Monomers. *Chem. Rev.* **2009**, *109*, S215–S244.
- (15) Zhang, W.; Waddell, P. M.; Tiedemann, M. A.; Padilla, C. E.; Mei, J.; Chen, L.; Carrow, B. P. Electron-Rich Metal Cations Enable Synthesis of High Molecular Weight, Linear Functional Polyethylenes. *J. Am. Chem. Soc.* **2018**, *140* (28), 8841–8850.
- (16) Chen, Z.; Leatherman, M. D.; Daugulis, O.; Brookhart, M. Nickel-Catalyzed Copolymerization of Ethylene and Vinyltrialkoxysilanes: Catalytic Production of Cross-Linkable Polyethylene and Elucidation of the Chain-Growth Mechanism. *J. Am. Chem. Soc.* **2017**, *139* (44), 16013–16022.
- (17) Leicht, H.; Göttker-Schnetmann, I.; Mecking, S. Synergetic Effect of Monomer Functional Group Coordination in Catalytic Insertion Polymerization. *J. Am. Chem. Soc.* **2017**, *139* (20), 6823–6826.
- (18) Diaz-Requejo, M. M.; Wehrmann, P.; Leatherman, M. D.; Trofimenko, S.; Mecking, S.; Brookhart, M.; Perez, P. J. Controlled, Copper-Catalyzed Functionalization of Polyolefins. *Macromolecules* **2005**, *38* (12), 4966–4969.
- (19) Aglietto, M.; Alterio, R.; Bertani, R.; Galleschi, F.; Ruggeri, G. Polyolefin functionalization by carbene insertion for polymer blends. *Polymer* **1989**, *30*, 1133–1136.
- (20) Shi, D.; Yang, J.; Yao, Z.; Wang, Y.; Huang, H.; Jing, W.; Yin, J.; Costa, G. Functionalization of isotactic polypropylene with maleic anhydride by reactive extrusion: mechanism of melt grafting. *Polymer* **2001**, *42* (13), 5549–5557.
- (21) Hopmann, C.; Adamy, M.; Cohnen, A. In *Reactive Extrusion*; Beyer, G., Hopmann, C., Eds.; Wiley-VCH Verlag GmbH & Co. KGaA: Weinheim, Germany, 2017; pp 1–10.
- (22) Gloor, P. E.; Tang, Y.; Kostanska, A. E.; Hamielec, A. E. Chemical modification of polyolefins by free radical mechanisms: a modelling and experimental study of simultaneous random scission, branching and crosslinking. *Polymer* **1994**, *35* (5), 1012–1030.
- (23) Lu, B.; Chung, T. C. Synthesis of maleic anhydride grafted polyethylene and polypropylene, with controlled molecular structures. *J. Polym. Sci., Part A: Polym. Chem.* **2000**, *38* (8), 1337–1343.
- (24) Zhang, M.; Colby, R. H.; Milner, S. T.; Huang, T.; deGroot, W.; Chung, T. C. M. Synthesis and Characterization of Maleic Anhydride Grafted Polypropylene with a Well-Defined Molecular Structure. *Macromolecules* **2013**, *46*, 4313–4323.
- (25) Hamielec, A. E.; Gloor, P. E.; Zhu, S. Kinetics of free radical modification of polyolefins in extruders – chain scission, crosslinking and grafting. *Can. J. Chem. Eng.* **1991**, *69* (3), 611–618.
- (26) Bettini, S. H. P.; Agnelli, J. A. M. Grafting of maleic anhydride onto polypropylene by reactive extrusion. *J. Appl. Polym. Sci.* **2002**, *85* (13), 2706–2717.
- (27) Porejko, S.; Gabara, W.; Kulesza, J. Grafting of maleic anhydride on polyethylene. II. Mechanism of grafting in a homogeneous medium in the presence of radical initiators. *J. Polym. Sci., Part A: Polym. Chem.* **1967**, *5* (7), 1563–1571.
- (28) He, X.; Zheng, S.; Huang, G.; Rong, Y. Solution Grafting of Maleic Anhydride on Low-Density Polyethylene: Effect on Crystallization Behavior. *J. Macromol. Sci., Part B: Phys.* **2013**, *52* (9), 1265–1282.
- (29) Ray, A.; Zhu, K.; Kissin, Y. V.; Cherian, A. E.; Coates, G. W.; Goldman, A. S. Dehydrogenation of aliphatic polyolefins catalyzed by pincer-ligated iridium complexes. *Chem. Commun.* **2005**, 3388–3390.
- (30) Bunescu, A.; Lee, S.; Li, Q.; Hartwig, J. F. Catalytic Hydroxylation of Polyethylenes. *ACS Cent. Sci.* **2017**, *3* (8), 895–903.
- (31) Boen, N. K.; Hillmyer, M. A. Selective and Mild Oxy-functionalization of Model Polyolefins. *Macromolecules* **2003**, *36* (19), 7027–7034.
- (32) Bae, C.; Hartwig, J. F.; Chung, H.; Harris, N. K.; Switek, K. A.; Hillmyer, M. A. Regiospecific Side-Chain Functionalization of Linear Low-Density Polyethylene with Polar Groups. *Angew. Chem., Int. Ed.* **2005**, *44* (39), 6410–6413.
- (33) Bae, C.; Hartwig, J. F.; Boen Harris, N. K.; Long, R. O.; Anderson, K. S.; Hillmyer, M. A. Catalytic Hydroxylation of Polypropylenes. *J. Am. Chem. Soc.* **2005**, *127* (2), 767–776.
- (34) Kondo, Y.; García-Cuadrado, D.; Hartwig, J. F.; Boen, N. K.; Wagner, N. L.; Hillmyer, M. A. Rhodium-Catalyzed, Regiospecific Functionalization of Polyolefins in the Melt. *J. Am. Chem. Soc.* **2002**, *124* (7), 1164–1165.
- (35) Foster, G. N.; Wasserman, S. H.; Yacka, D. J. Oxidation behavior and stabilization of metallocene and other polyolefins. *Angew. Makromol. Chem.* **1997**, *252*, 11–32.
- (36) Liu, D.; Bielawski, C. W. Direct azidation of isotactic polypropylene and synthesis of ‘grafted to’ derivatives thereof using azide–alkyne cycloaddition chemistry. *Polym. Int.* **2017**, *66* (1), 70–76.
- (37) Li, H.; Ma, P.; Chen, Y.; Zhou, H.; Huang, H.; Liu, L.; Li, L.; Plummer, C. M. Regioselective post-functionalization of isotactic polypropylene by amination in the presence of N-hydroxyphthalimide. *Polym. Chem.* **2019**, *10* (5), 619–626.
- (38) Zhou, H.; Wang, S.; Huang, H.; Li, Z.; Plummer, C. M.; Wang, S.; Sun, W. H.; Chen, Y. Direct Amination of Polyethylene by Metal-Free Reaction. *Macromolecules* **2017**, *50* (9), 3510–3515.
- (39) Coiai, S.; Augier, S.; Pinzino, C.; Passaglia, E. Control of degradation of polypropylene during its radical functionalisation with furan and thiophene derivatives. *Polym. Degrad. Stab.* **2010**, *95*, 298–305.
- (40) Moad, G.; Rizzardo, E.; Thang, S. H. Radical addition–fragmentation chemistry in polymer synthesis. *Polymer* **2008**, *49* (5), 1079–1131.
- (41) Chiefari, J.; Mayadunne, R. T. A.; Moad, C. L.; Moad, G.; Rizzardo, E.; Postma, A.; Skidmore, M. A.; Thang, S. H. Thiocarbonylthio Compounds (SC(Z)S-R) in Free Radical Polymerization with Reversible Addition-Fragmentation Chain Transfer (RAFT Polymerization). Effect of the Activating Group Z. *Macromolecules* **2003**, *36*, 2273–2283.
- (42) Mayadunne, R. T. A.; Rizzardo, E.; Chiefari, J.; Krstina, J.; Moad, G.; Postma, A.; Thang, S. H. Living Polymers by the Use of Trithiocarbonates as Reversible Addition-Fragmentation Chain Transfer (RAFT) Agents: ABA Triblock Copolymers by Radical Polymerization in Two Steps. *Macromolecules* **2000**, *33* (2), 243–245.
- (43) Mayadunne, R. T. A.; Rizzardo, E.; Chiefari, J.; Chong, Y. K.; Moad, G.; Thang, S. H. Living Radical Polymerization with Reversible Addition-Fragmentation Chain Transfer (RAFT Polymerization) Using Dithiocarbamates as Chain Transfer Agents. *Macromolecules* **1999**, *32* (21), 6977–6980.
- (44) Czaplyski, W. L.; Na, C. G.; Alexanian, E. J. C–H Xanthylation: A Synthetic Platform for Alkane Functionalization. *J. Am. Chem. Soc.* **2016**, *138* (42), 13854–13857.
- (45) Na, C. G.; Alexanian, E. J. A General Approach to Site-Specific, Intramolecular C–H Functionalization Using Dithiocarbamates. *Angew. Chem., Int. Ed.* **2018**, *57* (40), 13106–13109.
- (46) Smith, G. E. P.; Alliger, G.; Carr, E. L.; Young, K. C. Thiocarbonylsulfenamides. *J. Org. Chem.* **1949**, *14* (6), 935–945.
- (47) Gottfried, A. C.; Brookhart, M. Living Polymerization of Ethylene Using Pd(II)  $\alpha$ -Diimine Catalysts. *Macromolecules* **2001**, *34* (5), 1140–1142.
- (48) Williamson, J. B.; Czaplyski, W. L.; Alexanian, E. J.; Leibfarth, F. A. Regioselective C–H Xanthylation as a Platform for Polyolefin Functionalization. *Angew. Chem., Int. Ed.* **2018**, *57*, 6261–6265.
- (49) Plummer, C. M.; Zhou, H.; Zhu, W.; Huang, H.; Liu, L.; Chen, Y. Mild halogenation of polyolefins using an N-haloamide reagent. *Polym. Chem.* **2018**, *9* (11), 1309–1317.
- (50) Benkeser, R. A.; Hazdra, J. J. Factors Influencing the Direction of Elimination in the Chugaev Reaction. *J. Am. Chem. Soc.* **1959**, *81* (1), 228–231.
- (51) Betou, M.; Male, L.; Steed, J. W.; Grainger, R. S. Carbamoyl Radical-Mediated Synthesis and Semipinacol Rearrangement of  $\gamma$ -Lactam Diols. *Chem. - Eur. J.* **2014**, *20*, 6505–6517.

(52) Chugaev, L. A new method for the preparation of unsaturated hydrocarbons. *Ber. Dtsch. Chem. Ges.* **1899**, 32 (3), 3332–3335.

(53) Braunecker, W. A.; Matyjaszewski, K. Controlled/living radical polymerization: Features, developments, and perspectives. *Prog. Polym. Sci.* **2007**, 32 (1), 93–146.

(54) Zard, S. Z. In *Handbook of RAFT Polymerization*; Barner-Kowollik, C., Ed.; Wiley-VCH Verlag GmbH & Co. KGaA: Weinheim, Germany, 2008.

(55) Inoue, S.; Kumagai, T.; Tamezawa, H.; Aota, H.; Matsumoto, A.; Yokoyama, K.; Matoba, Y.; Shibano, M. Predominant methyl radical initiation preceded by  $\beta$ -scission of alkoxy radicals in allyl polymerization with organic peroxide initiators at elevated temperatures. *Polym. J.* **2010**, 42 (9), 716–721.

(56) Norrish, R. G. W.; Searby, M. H. The photochemical decomposition of dicumyl peroxide and cumene hydroperoxide in solution. *Proc. R. Soc. London A Math. Phys. Sci.* **1956**, 237 (1211), 464–475.

(57) Blanksby, S. J.; Ellison, G. B. Bond Dissociation Energies of Organic Molecules. *Acc. Chem. Res.* **2003**, 36 (4), 255–263.

(58) Roberts, B. Polarity-reversal catalysis of hydrogen-atom abstraction reactions: concepts and applications in organic chemistry. *Chem. Soc. Rev.* **1999**, 28 (1), 25–35.

(59) Hioe, J.; Zipse, H. Radical stability and its role in synthesis and catalysis. *Org. Biomol. Chem.* **2010**, 8 (16), 3609.

(60) Jeffery, J.; Ercole, F.; Mayadunne, R. T. A.; Moad, G.; Rizzardo, E.; Le, T. P. T.; Chiefari, J.; Krstina, J.; Chong, Y. K.; Moad, C. L.; Thang, S. H.; Meijs, G. F. Living Free-Radical Polymerization by Reversible Addition-Fragmentation Chain Transfer: The RAFT Process. *Macromolecules* **2002**, 31 (16), 5559–5562.

(61) Zard, S. Z. Some intriguing mechanistic aspects of the radical chemistry of xanthates. *J. Phys. Org. Chem.* **2012**, 25 (11), 953–964.

(62) Manning, S. C.; Moore, R. B. Carboxylation of Polypropylene by Reactive Extrusion With Functionalized Peroxides for Use as a Compatibilizer in Polypropylene/Polyamide-6,6 Blends. *J. Vinyl Addit. Technol.* **1997**, 3 (2), 184–189.

(63) Berzin, F.; Flat, J. J.; Vergnes, B. Grafting of maleic anhydride on polypropylene by reactive extrusion: effect of maleic anhydride and peroxide concentrations on reaction yield and products characteristics. *J. Polym. Eng.* **2013**, 33 (8), 673–682.

(64) Cicogna, F.; Coiai, S.; Passaglia, E.; Tucci, I.; Ricci, L.; Ciardelli, F.; Batistini, A. Grafting of functional nitroxyl free radicals to polyolefins as a tool to postreactor modification of polyethylene-based materials with control of macromolecular architecture. *J. Polym. Sci., Part A: Polym. Chem.* **2011**, 49 (1), 781–796.

(65) Assoun, L.; Manning, S. C.; Moore, R. B. Carboxylation of polypropylene by reactive extrusion with functionalised peroxides. *Polymer* **1998**, 39 (12), 2571–2577.